

MultiFIT: A Multivariate Multiscale Framework for Independence Tests

Shai Gorsky

Department of Statistical Science, Duke University

and

Li Ma*

Department of Statistical Science, Duke University

May 3, 2022

Abstract

We present a framework for nonparametrically testing the independence between two random vectors that is scalable to massive data both computationally and statistically. We take a multi-scale divide-and-conquer strategy by breaking down the multivariate test into univariate tests of independence on a collection of 2×2 contingency tables, constructed by sequentially discretizing the sample space from coarse to fine scales. This strategy transforms a nonparametric testing problem that traditionally requires quadratic computational complexity with respect to the sample size into one that scales almost linearly with the sample size. We further consider the scenario when the dimensionality of the random vectors grows large, in which case the curse of dimensionality demonstrates itself in our framework through an explosion in the number of univariate tests to be completed. To address this challenge we propose a data-adaptive coarse-to-fine testing procedure that completes a fraction of the univariate tests, which are judged to be prone to containing evidence for dependency by exploiting the spatial features of dependency structures. We provide a finite-sample theoretical guarantee for the exact validity of the adaptive procedure. In particular, we show that this procedure satisfies strong control of the family-wise error rate without any need for resampling or large-sample approximation, which existing approaches typically require. We demonstrate the substantial computational advantage of the procedure in comparison to existing approaches as well as its desirable statistical power under various dependency scenarios through an extensive simulation study. We illustrate through examples that our framework can be used not only for testing independence but for learning the nature of the underlying dependency. Finally, we demonstrate the use of our method through analyzing a data set from flow cytometry.

Keywords: Nonparametric inference, multiple testing, unsupervised learning, scalable inference, massive data

*LM's research is partly supported by NSF grants DMS-1612889 and DMS-1749789.

1 Introduction

The problem of testing whether or not two random variables are independent appears frequently in the analysis of multivariate data. Our focus herein lies on the case when one or both variables are multivariate (i.e., random vectors), and in particular when the number of observations can potentially be massive (e.g., millions or more). This ‘big data’ scenario presents a particular challenge to existing nonparametric independence tests, which typically require a computational complexity that scales at least quadratically with the sample size, making them impractical for massive data sets that are nowadays routinely generated in a variety of fields. In addition, we will allow the dimensionality of both random vectors to be moderately large, ranging up to about 100 dimensions each.

Testing independence and learning the dependency structure has been a fundamental statistical problem since the very beginning of modern statistics, and the last two decades have witnessed a surging of interest in this problem among statisticians, engineers and computer scientists. A variety of different methods have been proposed for testing independence between random vectors. For example, Székely and Rizzo (2009) generalize the product-moment covariance and correlation to the distance covariance and correlation. This generalization has an equivalent definition in terms of empirical characteristic functions. Bakirov et al. (2006), Fan et al. (2017), and Meintanis and Iliopoulos (2008) all developed nonparametric tests of independence based on the distance between the empirical joint characteristic function of the random vectors and the product of the marginal empirical characteristic functions of the two random vectors. Székely and Rizzo (2013) further consider an asymptotic scenario with the dimensionality of the vectors increasing to infinity while keeping the sample size fixed. In a different vein, Heller et al. (2013) form a test based on univariate tests of independence between the distances of each of the random vectors from a central point and perform inference based on permutations. In the machine learning literature, a class of kernel-based tests for independence have also become popular. For example, Gretton et al. (2008) form a test based on the eigenspectrum of covariance operators in a reproducing kernel Hilbert spaces (RKHS). More recently, Pfister et al. (2018) generalized this approach to the multivariate case by embedding the joint distribution into a RKHS. Most recently, Weihs et al. (2018) defined a class of multivariate nonparametric

measures which leads to multivariate extensions of the Bergsma-Dassios sign covariance. Aside from these methods that are applicable to multivariate random vectors, there are also a number of methods proposed for testing independence of univariate random variables nonparametrically, some notable examples, among many others, include Reshef et al. (2011), Wang et al. (2016), and Zhang (2017).

The existing multivariate independence tests generally require the computation of statistics at a computational complexity that scales at least quadratically in the sample size, making them impractical for data sets with massive sample sizes. We will illustrate this computational bottleneck in our numerical studies. Moreover, many of these multivariate methods also require resampling, in the form of either permutation or bootstrap, to complete inference such as evaluating the statistical significance. This additional computational burden makes practical applications of these methods very computationally expensive even for problems with moderate sample sizes. To overcome this difficulty, some works appeal to asymptotic approximations (either in large n or in large p) (Székely and Rizzo, 2013; Pfister et al., 2018) to derive procedures that when the asymptotic conditions are satisfied do not require resampling for inference.

In this work we aim to tackle the fundamental computational bottleneck in nonparametric multivariate independence testing through generalizing a ‘multi-scale divide-and-conquer’ strategy recently proposed for univariate independence testing by Ma and Mao (2018). Specifically, instead of calculating a single test statistic for independence all at once, our method breaks apart the nonparametric multivariate test of independence into simple univariate independence tests on a collection of 2×2 contingency tables defined by sequentially discretizing the original sample space at a cascade of scales. This approach transforms a complex nonparametric testing problem into a multiple testing problem that can be addressed with a computational complexity that scales almost linearly with the sample size.

In high-dimensional problems, the curse of dimensionality arises under this strategy through an explosion in the number of univariate independence tests needed to be completed. To address this challenge, we propose a data-adaptive coarse-to-fine sequential testing procedure, which exploits the spatial characteristics of dependency structures and completes a fraction of the univariate tests judged (based on statistical evidence on ‘ancestral’ tables)

to be prone to containing evidence for dependency. Inference (e.g., evaluating the statistical significance of the testing procedure) can then be completed based on multiple testing adjustment based on the resulting p -values from those univariate tests.

In contrast to other existing methods, which require resampling or asymptotics for guaranteeing their validity approximately, we provide a finite-sample theory that guarantees the *exact* validity of our data-adaptive procedure for any given sample size in terms of properly controlling the family-wise error rate (FWER) without resorting to either resampling or asymptotic approximation. Avoiding resampling is extremely important in applications to massive data where existing methods are often too slow to be completed even just once. A finite-sample theory brings the peace of mind that regardless of the sample size the procedure is valid. Moreover, we show through examples that our framework possesses the ability to identify the nature of the underlying dependency beyond just completing a hypothesis test on the null of independence.

We carry out extensive numerical studies to illustrate both the computational efficiency and statistical performance of our proposed approach in comparison to the state-of-the-art, and demonstrate its application to a data set from a flow cytometry experiment.

2 Method

In Section 2.1, we introduce some basic notions and notations that are necessary for describing our multi-scale divide-and conquer testing framework. In Section 2.2, we will describe our data-adaptive testing procedure and establish a finite-sample theoretical guarantee.

2.1 A Multi-scale Divide-and-Conquer Framework

Without loss of generality, let $\Omega = [0, 1]^D$ be our sample space. (Our formulation will also apply more generally when some of the D dimensions of Ω are ordered categorical.) Let $\mathbf{Z} = (Z_1, \dots, Z_D)$ be a random vector with a joint D -variate probability distribution F on the sample space Ω . **Figure 1** provides an illustration of the key concepts introduced in this section. First, we define a sequence of nested partitions on each of the D margins of Ω . (For expositional simplicity, throughout the work we will focus on dyadic recursive

partitions on the margins of Ω , though our framework applies generally to any sequence of nested partitions that generate the Borel σ -algebra.)

Definition 2.1. *Level- k Marginal Dyadic Partition:*

\mathcal{P}^k is a *level- k marginal dyadic partition* if $\mathcal{P}^k = \{[\frac{l-1}{2^k}, \frac{l}{2^k})\}_{l \in \{1, \dots, 2^k\}}$.

A D -dimensional cuboid may be formed by taking the Cartesian product of one interval from each of the D marginal partitions, and we further consider the collection of all such cuboids with any $\mathbf{k} = (k_1, \dots, k_D) \in \mathbb{N}_0^D$ specifying the level of each dimension:

Definition 2.2. *\mathbf{k} -Cuboid:*

For any $\mathbf{k} = (k_1, \dots, k_D) \in \mathbb{N}_0^D$, we call a set $A \subset \Omega$ a *\mathbf{k} -cuboid* if it is of the form

$$A = A_1 \times A_2 \times \dots \times A_D, \quad \text{with } A_d \in \mathcal{P}^{k_d} \text{ for all } d = 1, 2, \dots, D.$$

That is, a \mathbf{k} -cuboid is determined by some $\mathbf{l} = (l_1, \dots, l_D)$ with each $1 \leq l_d \leq 2^{k_d}$:

$$A = \times_{d \in \{1, \dots, D\}} \left[\frac{l_d - 1}{2^{k_d}}, \frac{l_d}{2^{k_d}} \right).$$

Definition 2.3. *\mathbf{k} -Stratum:*

For any $\mathbf{k} = (k_1, \dots, k_D) \in \mathbb{N}_0^D$, we call the collection of all \mathbf{k} -cuboids the *\mathbf{k} -stratum*, which is

$$\mathcal{A}^{\mathbf{k}} = \mathcal{P}^{k_1} \times \dots \times \mathcal{P}^{k_D}.$$

Further, we call $|\mathbf{k}| = \sum_{d=1}^D k_d$ the *resolution* of the \mathbf{k} -stratum. We also say that a \mathbf{k} -cuboid is of resolution r when $|\mathbf{k}| = r$. Accordingly, if for $\mathbf{k}, \mathbf{k}' \in \mathbb{N}_0^D$, $|\mathbf{k}| = |\mathbf{k}'|$, then we say the \mathbf{k} -stratum is of the same resolution as the \mathbf{k}' -stratum. Similarly, if $|\mathbf{k}| < |\mathbf{k}'|$, then the \mathbf{k} -stratum is of *lower* resolution than the \mathbf{k}' -stratum, or equivalently that latter is of *higher* resolution. Also, we from now on denote $\mathbf{k}' \geq \mathbf{k}$ if $k'_1 \geq k_1, k'_2 \geq k_2, \dots, k'_D \geq k_D$. We denote $\mathbf{k}' > \mathbf{k}$ if $\mathbf{k}' \geq \mathbf{k}$ and there exists $d \in \{1, \dots, D\}$ such that $k'_d > k_d$. If $\mathbf{k}' \geq \mathbf{k}$ we say that $\mathcal{A}^{\mathbf{k}'}$ is a *finer stratum* than $\mathcal{A}^{\mathbf{k}}$, which is said to be a *coarser stratum*. Note that if $\mathcal{A}^{\mathbf{k}'}$ is finer than $\mathcal{A}^{\mathbf{k}}$ then $|\mathbf{k}'|$ is higher than $|\mathbf{k}|$. However, the opposite does not necessarily hold.

Our goal is to test the independence of two random vectors. From now on then, let us consider testing the independence between the first D_x elements of \mathbf{Z} with the other

$D_y = D - D_x$. That is, let $\mathbf{Z} = (\mathbf{X}, \mathbf{Y})$ where $\mathbf{X} \in [0, 1]^{D_x}$ and $\mathbf{Y} \in [0, 1]^{D_y}$. We next define a discretized form of independence which we will show in Theorem 2.1 fully characterizes the multivariate independence:

Definition 2.4. *\mathbf{k} -independence:*

For any $A \in \mathcal{A}^{\mathbf{k}}$, we can write $A = A_x \times A_y$ where

$$A_x = \bigtimes_{d=1}^{D_x} \left[\frac{l_d - 1}{2^{k_d}}, \frac{l_d}{2^{k_d}} \right) \quad \text{and} \quad A_y = \bigtimes_{d=D_x+1}^D \left[\frac{l_d - 1}{2^{k_d}}, \frac{l_d}{2^{k_d}} \right).$$

We say that \mathbf{X} and \mathbf{Y} are *\mathbf{k} -independent* and write it as $\mathbf{X} \perp_{\mathbf{k}} \mathbf{Y}$ if for any $A \in \mathcal{A}^{\mathbf{k}}$,

$$\mathbb{P}(\mathbf{X} \in A_x, \mathbf{Y} \in A_y) = \mathbb{P}(\mathbf{X} \in A_x) \cdot \mathbb{P}(\mathbf{Y} \in A_y).$$

Theorem 2.1.

$$\mathbf{X} \perp \mathbf{Y} \Leftrightarrow \mathbf{X} \perp_{\mathbf{k}} \mathbf{Y} \quad \text{for all } \mathbf{k} \in \mathbb{N}_0^D.$$

We next define a collection of log odd ratios (LORs), each corresponding to the division of one of the $D_x \times D_y$ faces of a \mathbf{k} -cuboid A into four quadrants. In Theorem 2.2 we show how these LORs characterize \mathbf{k} -independency.

Definition 2.5. *(i, j) -quadrants of a \mathbf{k} -cuboid:*

For every \mathbf{k} -cuboid $A \in \mathcal{A}^{\mathbf{k}}$ and $i, j \in \{1, \dots, D\}$, one can partition A into four blocks by dividing A in the (i, j) th face (that is, the side of A spanned by the i th and j th dimensions) into four quadrants while keeping the other dimensions intact.

$$A = A_{ij}^{00} \sqcup A_{ij}^{01} \sqcup A_{ij}^{10} \sqcup A_{ij}^{11},$$

where for $a, b \in \{0, 1\}$,

$$A_{ij}^{ab} = \bigtimes_{d=1}^D \begin{cases} \left[\frac{2l_d - 2 + a}{2^{k_d+1}}, \frac{2l_d - 1 + a}{2^{k_d+1}} \right) & \text{if } d = i \\ \left[\frac{2l_d - 2 + b}{2^{k_d+1}}, \frac{2l_d - 1 + b}{2^{k_d+1}} \right) & \text{if } d = j \\ \left[\frac{l_d - 1}{2^{k_d}}, \frac{l_d}{2^{k_d}} \right) & \text{if } d \in \{1, \dots, D\} \setminus \{i, j\} \end{cases}.$$

Definition 2.6. *(i, j) -face log odds ratio of a \mathbf{k} -cuboid:*

For any \mathbf{k} -cuboid $A \in \mathcal{A}^{\mathbf{k}}$, $1 \leq i \leq D_x$, and $D_x < j \leq D$, we call $\theta_{ij}(A) = \log \frac{F(A_{ij}^{00}) \cdot F(A_{ij}^{11})}{F(A_{ij}^{01}) \cdot F(A_{ij}^{10})}$ the *(i, j) -face log odds ratio (LOR)* of the \mathbf{k} -cuboid A .

The following lemma shows that if \mathbf{X} and \mathbf{Y} are \mathbf{k} -independent, they are also independent on all coarser strata. This will enable our coarse-to-fine scanning test strategy we present in Section 2.2.

Lemma 2.1. *If $\mathbf{X} \perp_{\mathbf{k}} \mathbf{Y}$ then $\mathbf{X} \perp_{\mathbf{k}'} \mathbf{Y}$ for all $\mathbf{k}' \leq \mathbf{k}$.*

Definition 2.7. *(i, j) -face coarser strata:*

Given $\mathbf{k} \in \mathbb{N}_0^D$ and $i, j \in \{1, \dots, D\}$ denote

$$\mathbf{k}[i, j] = \{\mathbf{k}' \in \mathbb{N}_0^D : k'_i < k_i, k'_j < k_j \text{ and } k'_d = k_d \text{ for all } d \in \{1, \dots, D\} \setminus \{i, j\}\}$$

and let then

$$\mathcal{A}^{\mathbf{k}[i, j]} = \bigcup_{\mathbf{k}' \in \mathbf{k}[i, j]} \mathcal{A}^{\mathbf{k}'}$$

be the union of all strata that are coarser than the stratum $\mathcal{A}^{\mathbf{k}}$ on the (i, j) -face of A .

Our next theorem ties the \mathbf{k} -independence of the random vectors \mathbf{X} and \mathbf{Y} with the (i, j) -face LORs:

Theorem 2.2. *For any $\mathbf{k} > \mathbf{0}_D$*

$$\begin{aligned} \mathbf{X} \perp_{\mathbf{k}} \mathbf{Y} &\Leftrightarrow \theta_{ij}(A) = 0 \\ &\forall i \in \{1, 2, \dots, D_x\}, \quad j \in \{D_x + 1, \dots, D\}, \quad A \in \mathcal{A}^{\mathbf{k}[i, j]}. \end{aligned}$$

We are now ready to articulate the main problem at hand: testing the null hypothesis $H_0 : \mathbf{X} \perp \mathbf{Y}$ vs. the alternative $H_1 : \textit{otherwise}$.

Our aim is to utilize tests on the LORs for the 2×2 tables that discretize the data at different resolutions. To this end, we first define the counts of data points in each cuboid:

Definition 2.8. *Cuboid Counts:*

Suppose $\mathbf{Z}_1, \dots, \mathbf{Z}_n$ are i.i.d draws from F . Then for any $A \in \mathcal{A}^{\mathbf{k}}$, let $n(A)$ be the number of observations in A . That is, $n(A) = |\{c : \mathbf{Z}_c \in A\}|$.

Next, we define the 2×2 contingency tables on which we will apply standard univariate tests of independence in order to test for $\theta_{ij}(A) = 0$.

Definition 2.9. (i, j) -table of a \mathbf{k} -cuboid:

With an i.i.d. sample from F , for any $A \in \mathcal{A}^{\mathbf{k}}$ and $i, j \in \{1, \dots, D\}$, we call the 2×2 contingency table given by

$$\mathbf{n}_{ij}(A) = \{n(A_{ij}^{00}), n(A_{ij}^{01}), n(A_{ij}^{10}), n(A_{ij}^{11})\} \quad \text{or} \quad \begin{array}{|c|c|} \hline n(A_{ij}^{00}) & n(A_{ij}^{01}) \\ \hline n(A_{ij}^{10}) & n(A_{ij}^{11}) \\ \hline \end{array}$$

the (i, j) -table of A .

See **Figure 1** for an illustration of the above definitions. Combining all of the above definitions with Theorem 2.1, Lemma 2.1, and Theorem 2.2, we get the main thrust of the coarse-to-fine strategy in our framework: start by testing for the null that all of the (i, j) -face LORs are 0 for the cuboid at resolution 0 (the entire sample space), and continue to test cuboids in higher and higher resolutions. In theory, one needs infinitely many observations in order to test the right hand side of Theorem 2.2. With finite samples, one should only test for whether the LOR is 0 on tables with a minimum number of observations in each row and column and/or on cuboids up to some maximal resolution r as cuboids at higher resolutions will eventually be containing too few, if any, observations to allow reliable inference on the corresponding LORs. In practice, one can let the maximal resolution grow logarithmically with the sample size.

2.2 The MultiFIT Procedure

Our testing procedure is based on a coarse-to-fine multiple testing strategy. First, we note that if one were to exhaustively test independence on all possible 2×2 tables of all cuboids up to a moderate level of resolution levels, the number of tests required would quickly become massive as the dimensionality of the sample space grows. Suppose the dimensionality of \mathbf{X} is D_x , the dimensionality of \mathbf{Y} is D_y , $D = D_x + D_y$ and let $r = |\mathbf{k}|$. In a given \mathbf{k} -stratum there are 2^r \mathbf{k} -cuboids. Further, in a resolution r there are $\binom{r+D-1}{D-1}$ strata (the number of non-commutative ways to form the sum r from D non-negative integers). For each cuboid we need to test the LOR on $D_x \times D_y$ (i, j) -faces. Thus, if one were to exhaustively test all cuboids up to resolution r we need to perform $\sum_{\rho=0}^r D_x \cdot D_y \cdot 2^\rho \cdot \binom{\rho+D-1}{D-1}$ tests. For example, with $D_x = 40$, $D_y = 40$, one would have to perform $1.85 \cdot 10^{38}$ tests up

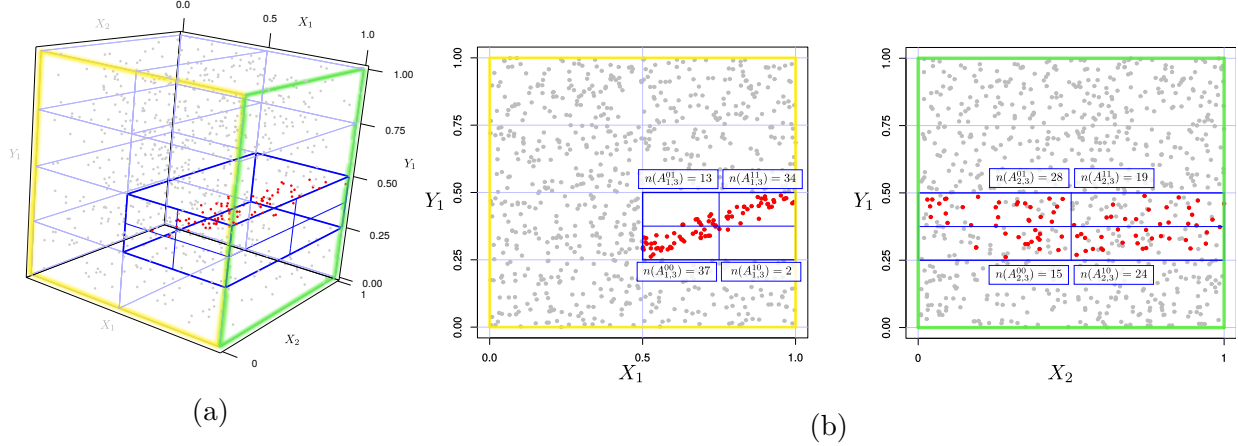


Figure 1: Illustration of the key concepts.

(a) A 3D view of a \mathbf{k} -cuboid and a \mathbf{k} -stratum where $\mathbf{X} = (X_1, X_2) = (Z_1, Z_2)$ and $\mathbf{Y} = Y_1 = Z_3$ (i.e. $D_x = 2$ and $D_y = 1$). The thin blue lines delineate all \mathbf{k} -cuboids with $\mathbf{k} = (1, 0, 2)$. The thick blue lines delineate the cuboid A for which $\mathbf{l} = (2, 1, 2)$, i.e., $A = ([0.5, 1) \times [0, 1)) \times [0.25, 0.5)$. The grey points are all data points outside of A , the red points are inside A .

(b) 2D views of the $(1, 3)$ -face (spanned by the X_1 and Y_1 margins) and the $(2, 3)$ -face of A (spanned by the X_2 and Y_1 margin). Left: Testing the null $\theta_{1,3}(A) = 0$, using the 2×2 table $\mathbf{n}_{1,3}(A) = (37, 13, 2, 34)$. Right: testing the null $\theta_{2,3}(A) = 0$ using the 2×2 table $\mathbf{n}_{2,3}(A) = (15, 28, 24, 19)$.

to a maximum resolution of 4. One may alleviate the problem by carrying out tests on tables whose column and row marginal totals exceed a threshold, for otherwise the table cannot have generated a statistically significant result anyway. Such a sample size screening is always recommended. However, with a substantial sample size, this alone will not suffice to reduce the number of tests to a tractable one when the number of dimensions is large. Beyond the consideration of computational practicality, reducing the number of tests is also desirable for the sake of statistical performance. Specifically, for every additional test we carry out there is a price to pay in multiple testing control, and thus it is important to be discreet in choosing the tests to complete.

Given these considerations, data-adaptive strategies are necessary for building practical testing procedures to deal with high dimensionality. We propose one such strategy by

completing the tests on tables that are ‘descendants’ of the tables in coarser strata that have generated p -values passing a pre-specified threshold. This strategy is motivated by the spatial characteristics of dependency structures—when \mathbf{X} and \mathbf{Y} are dependent, then nearby and nested cuboids tend to contain empirical evidence for the dependency in a correlated manner. Thus using the statistical evidence at coarser strata to inform the cuboids to test on in higher resolutions can lead to effective detection of the dependency structure.

We now are ready to present the adaptive testing procedure. Throughout the algorithm, we let $\mathcal{C}^{(r)}$ denote the collection of cuboids at resolution r on which we carry out independence tests over all of its $D_x \times D_y$ faces. Let R^* denote a resolution up to which the testing will be performed exhaustively on all cuboids and let R_{max} denote the maximum resolution at which the procedure will be terminated. The procedure is as follows:

- (0) **Initialization:** Let $\mathcal{C}^{(r)}$ be the collection of all cuboids of resolution r for $r = 0, 1, 2, \dots, R^*$, and let $\mathcal{C}^{(r)} = \emptyset$ for $R^* < r \leq R_{max}$.
- (1) Then for $r = 0, 1, 2, \dots, R_{max}$ do the following
 - 1a. **Independence testing:** Apply Fisher’s exact test of independence to the $D_x \cdot D_y$ (i, j) -tables of each cuboid $A \in \mathcal{C}^{(r)}$ and record the p -values.
 - 1b. **Selection of cuboids to test for the next resolution:** When $R^* \leq r < R_{max}$, if the (i, j) -table for a cuboid $A \in \mathcal{C}^{(r)}$ has a p -value more significant than a threshold p^* , add to $\mathcal{C}^{(r+1)}$ the four *child cuboids* of A generated from halving A along the i th and the j th margins respectively, each generating two children. (See **Figure 2** for an illustration.)
- (2) **Multiple testing control:** Apply any multiple testing procedure that provides strong FWER control at a given level α based on the p -values. Some examples include Holm’s step-down procedure (Holm, 1979), or a modified Holm method by Zhu and Guo (2017).

We present the pseudo-code for this procedure as Algorithm 1. For each cuboid A , we use $\mathbf{n}_{ij}(A)$ to represent the corresponding 2×2 (i, j) -table. The p -values for the cuboids selected in the `MultiFIT` procedure are computed according to the (central) hypergeometric null distributions of $\mathbf{n}_{ij}(A)$ given the marginal totals $n(A_{ij}^0)$, $n(A_{ij}^1)$, $n(A_{ij}^0)$, and $n(A_{ij}^1)$.

Algorithm 1 MultiFIT procedure for testing multivariate independence

Let $\mathcal{C}^{(r)}$ be the collection of all cuboids of resolution r for $r = 0, 1, 2, \dots, R^*$, and let $\mathcal{C}^{(r)} = \emptyset$ for $r = R^* + 1, \dots, R_{max}$. ▷ Step 0: Initialization

for r in $0, 1, 2, \dots, R_{max}$ **do** ▷ For each resolution

for each $A \in \mathcal{C}^{(r)}$ **do** ▷ For each cuboid selected for testing

for i in $1, 2, \dots, D_x$ **do**

for j in $1, 2, \dots, D_y$ **do**

 Apply Fisher's exact test on the (i, j) -table of A and record the p -value

▷ Step 1a: Independence testing

if $R^* \leq r < R_{max}$ **then**

if the (i, j) -table of A has a p -value smaller than a threshold p^* **then**

 Add the four half cuboids of A into $\mathcal{C}^{(r+1)}$

▷ Step 1b: Select cuboids for testing in the next resolution

end if

end if

end for

end for

end for

end for

Apply a multiple testing procedure that provides strong FWER control based on the recorded p -values. ▷ Step 2: Multiple testing control

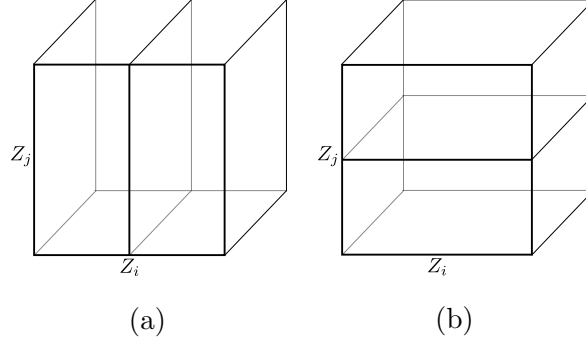


Figure 2: Parent and Children Cuboids: in (a) a cuboid is divided along the i^{th} margin to form two child cuboids and in (b) the same cuboid divided along the j^{th} margin to form two child cuboids.

At first glance, these null distributions appear to ignore the selection of a cuboid A based on the evidence in its ancestral cuboids. As such, one may suspect whether such p -values are still valid, i.e., stochastically larger than a uniform random variable under the null hypothesis of independence. The following theorem and corollary resolve this concern by showing that the distribution of $\mathbf{n}_{ij}(A)$ given the marginal totals is independent of the event that the cuboid A is selected in the procedure, and hence the p -values computed in the procedure are indeed still valid despite the adaptive selection. Consequently, one can control for FWER on the entire procedure using these p -values.

Theorem 2.3. *For any cuboid A , the conditional distribution of the (i, j) -table, $\mathbf{n}_{ij}(A)$, given the corresponding marginal totals $n(A_{ij}^{0:})$, $n(A_{ij}^{1:})$, $n(A_{i:}^{0:})$, and $n(A_{i:}^{1:})$, is the same central hypergeometric distribution when $\mathbf{X} \perp\!\!\!\perp \mathbf{Y}$ whether or not we condition on the event that A is selected in the MultiFIT procedure.*

Corollary 2.1. *The p -values computed during Step (1) of the MultiFIT procedure are valid, and thus Step (2) of the procedure can control FWER at any given level α .*

Remark: The above Corollary provides a *finite-sample* theoretical guarantee that MultiFIT attains exact control of the FWER regardless of the sample size n . This is an important property of our procedure in that for high-dimensional sample spaces traditional large n asymptotic controls of FWER can often be inaccurate, and existing methods typically appeal to resampling strategies such as permutation to provide actual finite-sample approximate

control of the FWER. But permutation is often computationally prohibitive in this context in that even just a single run of a test can be expensive, not to mention applying the same test hundreds to thousands of times. In contrast, `MultiFIT` achieves exact control of FWER by a single run of the procedure without resampling.

While the `MultiFIT` procedure guarantees FWER control, the p-value threshold p^* and the resolution threshold for exhaustive testing R^* will affect the number of tests the algorithm performs (and hence its computational time) as well as the power of the procedure. A smaller value for R^* will favor the detection of more global signals, while a larger R^* will favor localized signals. In our software, the default value for R^* is one - guaranteeing complete coverage of all cuboids at resolution one. The larger p^* is, the more tests will be performed (if $p^* = 1$, the test will run exhaustively). The default value set for p^* in our implementation is $(D_x \cdot D_y \cdot \log_2(n))^{-1}$. This reflects the need to be prudent about the number of tests that will be performed: our selection of p^* corresponds to choosing (on average) one parent test per resolution under the null hypothesis ($(D_x \cdot D_y)^{-1}$ term) and further restricts the threshold with the $(\log_2(n))^{-1}$ term so that presence of strong signals in large data will not lead to an explosion in the number of tests performed.

3 Numerical Examples

3.1 Computational Scalability

Before we examine the statistical performance of `MultiFIT`, we compare its computational scalability with those of three other methods—the Heller-Heller-Gorfine (HHG) multivariate test of association from Heller et al. (2013), the Distance Covariance (DCov) method of Székely and Rizzo (2009) and the kernel based method (dHSIC) of Pfister et al. (2018), which at the time of the writing are generally considered the state-of-the-art.

Figure 3 presents the computational time as the number of observations and dimensionality grow. All methods were run on the same computer, and for the three competitors were run until different sample sizes until they surpass the memory available. `MultiFIT` did not cause memory overflow at all the sample sizes tested. For `MultiFIT` we present the average duration of 20 executions for Fisher’s exact test with Holm’s correction under

two scenarios. The first scenario is for data generated under the null hypothesis, where all margins are drawn independently from a standard normal distribution. The second is where a margin of \mathbf{Y} is strongly linearly related to a margin of \mathbf{X} (the ‘linear’ scenario from Table 1 with $l = 3$). A property of **MultiFIT** is that when a signal is stronger more tests will pass the p -value threshold.

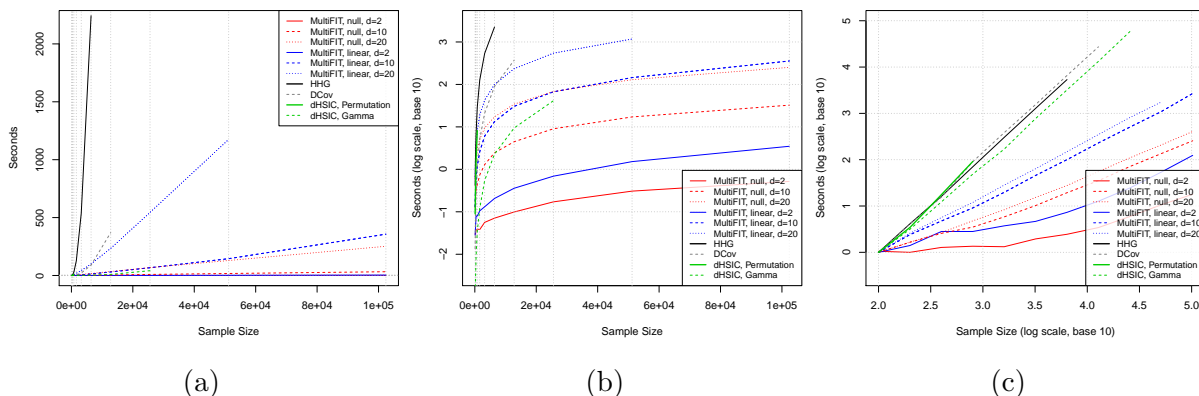


Figure 3: Computational scalability: a comparison of HHG, DCov, dHSIC (all with 1,000 permutations) and **MultiFIT** with $D_x = D_y = d$. (3a) run-time vs. sample size. (3b) log run-time vs. sample size for improved readability. (3c) log runtime versus log sample size, with the minimal logarithm of run-time subtracted to facilitate comparison of the slopes. Note that **MultiFIT** does not require permutation for exact FWER control. The dHSIC with Gamma approximation does not require permutation for approximate FWER control. The rest of the methods requires permutations for FWER control.

In summary, **MultiFIT** shows excellent scalability in sample size: as low as approximately $\mathcal{O}(n \log n)$ (including multiple testing adjustment). HHG, DCov and dHSIC without the Gamma approximation scale approximately $\mathcal{O}(n^2)$ in the number of observations. The Gamma approximation method of dHSIC may be faster in the presence of a strong signal, yet still cannot handle the larger sample sizes due to memory requirements. All of the methods except **MultiFIT** are roughly invariant to the dimensionality. However, as we shall see in Section 3.2, this invariance comes with a cost in power, whereas **MultiFIT** requires more testing with higher dimensions, but retains good power. It is also worth noting that with the Gamma approximation dHSIC loses its theoretical guarantee on inference validity, which our approach maintains.

3.2 Power

We next examine the statistical power of the competing methods under the following simulation settings. For $\mathbf{X} = (X_1, X_2)$ and $\mathbf{Y} = (Y_1, Y_2)$, we let X_1 and Y_1 be independently normally distributed, whereas X_2 and Y_2 are dependent according to several different scenarios, as illustrated in **Figure 4** and detailed in **Table 1**. We performed 2000 simulations for each scenario and at each of 20 noise levels, all with an FWER level of 0.05. **MultiFIT** scales the data with a marginal rank transformation by default, thereby bisecting the margins at resolution 0 along their medians. In order to provide a fair comparison, we first applied a rank transform to each of the D margins for every simulated data set as three competitors **HHG**, **DCov** and **dHSIC** performed much more poorly without the marginal rank transform.

In the execution of **MultiFIT** we utilize Fisher’s exact test the multiple testing adjustment of Zhu and Guo (2017). Notice that in the ‘circle’, ‘checkerboard’ and ‘local’ scenarios the cell counts at resolution 0 will be roughly equal. For all scenarios except the ‘local’, we set the tuning parameter R^* to 2, and for the ‘local’ scenario, where a signal is embedded in a small sub-portion of the margins X_2 and Y_2 and all other regions are independent, we applied the algorithm we set $R^* = 4$ to ensure exhaustive coverage up to resolution 4, and from there on continue only with tests whose p -value is below the default threshold for each of the higher resolutions.

MultiFIT outperforms **HHG**, **DCov** and **dHSIC** for the ‘sin’, ‘circle’, ‘checkerboard’ and ‘local’ scenarios, the cases that are richer with local structures. The picture is different in the ‘linear’ and ‘parabolic’ scenarios: they are ‘more global’, and there **HHG** and **dHSIC** outperform our algorithm (where **DCov** does so only in the ‘linear’ case). This is explained by the fact that the signal is observable almost entirely in the coarsest level, and as we go into higher resolutions we merely add insignificant tests that reduce the overall power.

Table 2 presents the results from a power simulation at 0.05 level for a high dimensional ‘linear’ scenario where both variables are of 40 dimensions. This example shows that although the computational complexity of the competing methods is invariant to the number of dimensions their performance in higher dimensions may be hindered compared to **MultiFIT**.

Table 1: Simulation Scenarios

Scenario	# of Data Points	Maximal Resolution	Simulation Setting
Sin	300	4	$X_1 = Z, Y_1 = Z', X_2 = U,$ $Y_2 = \sin(5\pi \cdot X_2) + 4\epsilon$
Circular	300	4	$X_1 = Z, Y_1 = Z',$ $X_2 = \cos(\theta) + \epsilon, Y_2 = \sin(\theta) + \epsilon'$
Checkerboard	500	5	$X_1 = Z, Y_1 = Z', X_2 = W + \epsilon,$ $Y_2 = \begin{cases} V_1 + \epsilon', & \text{if } W \text{ is odd} \\ V_2 + \epsilon', & \text{if } W \text{ is even} \end{cases}$
Linear	300	4	$X_1 = Z, Y_1 = Z', X_2 = U,$ $Y_2 = X_2 + 3\epsilon$
Parabolic	300	4	$X_1 = Z, Y_1 = Z', X_2 = U,$ $Y_2 = (X_2 - 0.5)^2 + 0.75\epsilon$
Local	1000	6	$X_1 = Z, Y_1 = Z', X_2 = Z'',$ $Y_2 = \begin{cases} X_2 + 1/6 \cdot \epsilon & \text{if } 0 < X_2, Z''' < 0.7 \\ Z''', & \text{otherwise} \end{cases}$

Six simulation scenarios. In all cases, Z, Z' are i.i.d $N(0, 1)$. At each noise level $l = 1, 2, \dots, 20$, ϵ, ϵ' and ϵ'' are i.i.d $N(0, (l/20)^2)$, and the following random variables are all independent: $U \sim \text{Uniform}(0, 1)$, $\theta \sim \text{Uniform}(-\pi, \pi)$, $W \sim \text{Multi-Bern}(\{1, 2, 3, 4, 5\}, (1/5, 1/5, 1/5, 1/5, 1/5))$, $V_1 \sim \text{Multi-Bern}(\{1, 3, 5\}, (1/3, 1/3, 1/3))$, $V_2 \sim \text{Multi-Bern}(\{2, 4\}, (1/2, 1/2))$ and Z'', Z''' are i.i.d $N(0, 1)$. The maximal resolution is the algorithm's default: $\lceil \log_2(n/10) \rceil$ where n is the number of data points. In all cases we apply the screening rule that only tests pairs of margins if the grand total is at least 25, and all four marginal totals are at least 10.

Table 2: High dimensional example

MultiFIT: mid- p correction	HHG: sum χ^2	HHG: sum likelihood	HHG: mean χ^2	HHG: mean likelihood	DCov	DHSIC: Permutation	DHSIC: Gamma
0.970	0.112	0.102	0.056	0.048	0.468	0.456	0.348

Simulated power: 500 simulations, $D_x = D_y = 40$, $X_1, \dots, X_{39}, Y_1, \dots, Y_{39}$ are i.i.d. $N(0, 1)$, $X_{40} \sim U(0, 1)$ and $Y_{40} = X_{40} + 3\epsilon$ where $\epsilon \sim N(0, (3/20)^2)$

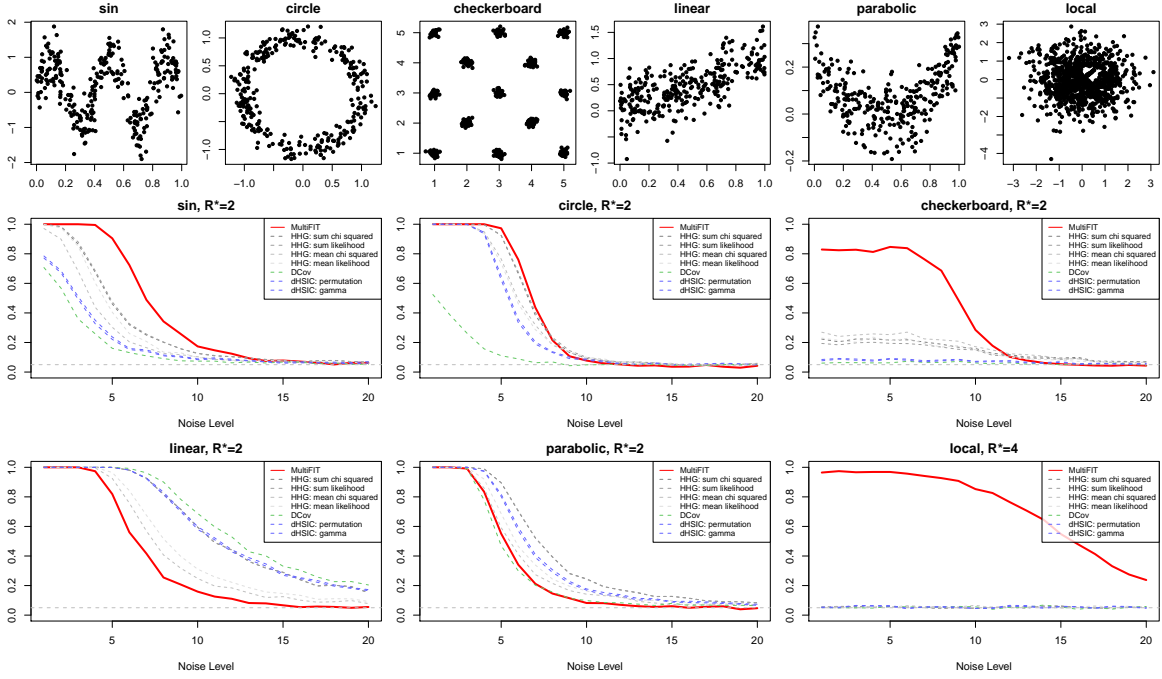


Figure 4: A comparison of simulated power.

Top row: dependent margins of scenarios with noise level 2. Bottom rows: estimated power

3.3 Additional Examples

In this section we provide two examples that highlight MultiFIT's unique ability of learning the dependency structure in the data. The examples in the previous sections focused on demonstrating our algorithm on signals that are mainly marginal. Here, we broaden the canvas.

Example 3.3.1. A Rotated Circle:

In this scenario, we take \mathbf{X} and \mathbf{Y} to be each of three dimensions, with 800 data points.

We first generate a ‘circle’ scenario so that $X_1, Y_1, X_2,$ and Y_2 are all i.i.d. standard normals. Take $X_3 = \cos(\theta) + \epsilon, Y_3 = \sin(\theta) + \epsilon'$ where ϵ and ϵ' are i.i.d $N(0, (1/10)^2)$ and $\theta \sim \text{Uniform}(-\pi, \pi)$. We then rotate the circle by $\pi/4$ degrees in the X_2 - X_3 - Y_3 space by applying:

$$\begin{bmatrix} \cos(\pi/4) & -\sin(\pi/4) & 0 \\ \sin(\pi/4) & \cos(\pi/4) & 0 \\ 0 & 0 & 1 \end{bmatrix} \begin{bmatrix} | & | & | \\ X_2 & X_3 & Y_3 \\ | & | & | \end{bmatrix}$$

The rotated circle is harder to see by examining the margins. See **Figure 5** for the marginal views of the original and the rotated setting. **Figure 6** shows the tests our method identified with modified Holm’s adjusted p -values below 0.001.

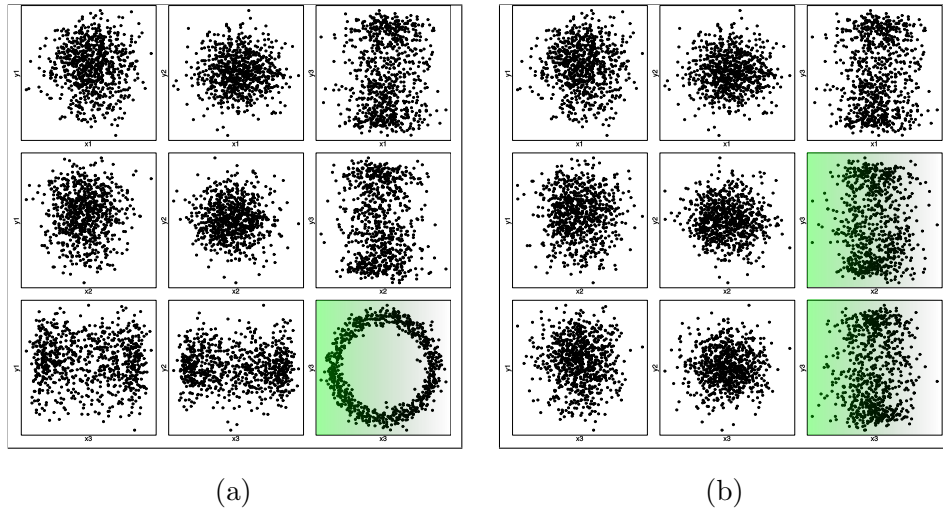


Figure 5: Marginal views of a circle and a rotated circle in a 3×3 setting. The signal in the original setting (a) is easily visible in the marginal view. Once rotated, the signal is spread between more margins, and harder to detect with the naked eye (b).

Example 3.3.2. Superimposed Sine Waves:

In this scenario, we follow the suggestion by Reshef et al. (2011) and examine our algorithm’s ability to (i) detect a signal that is made of two sine waves in different frequencies, and (ii) given a third dimension that determines which data points belong to which wave, to see if our algorithm successfully identifies this relation.

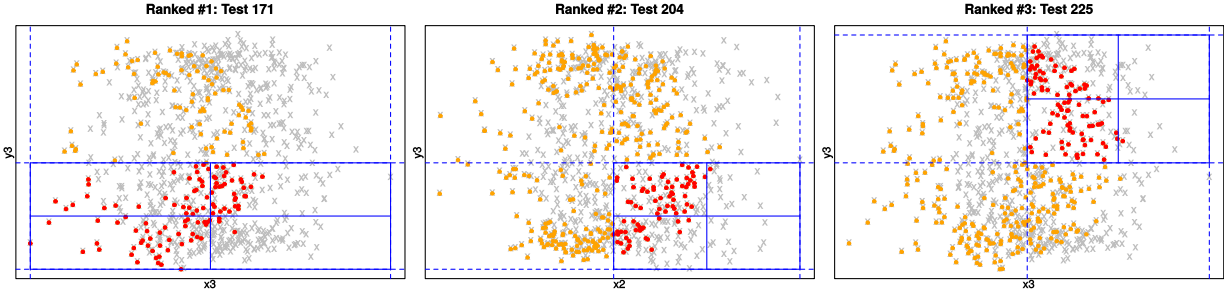


Figure 6: Tests for the rotated circle with modified Holm’s adjusted p -values below 0.001. The testing was performed with Fisher’s exact test on each 2×2 table with the default tuning parameters. The tests ranking #1 and #3 are in the X_3 - Y_3 plane, and are conditioned on X_2 , and the second ranking test is in the X_2 - Y_3 plane.

We take \mathbf{X} to be a two dimensional random variable and \mathbf{Y} to be one dimensional, all with 600 data points. Define $X_1 \sim U(0, 1)$, $X_2 \sim \text{Beta}(0.3, 0.3)$ independent of X_1 , and define:

$$Y = \begin{cases} \sin(10 \cdot X_1) + \epsilon, & \text{if } X_2 > 0.5 \\ \sin(40 \cdot X_1) + \epsilon, & \text{if } X_2 \leq 0.5 \end{cases}$$

See **Figure 7** for the marginal views of the superimposed setting. **Figure 8** shows the tests our method identified, which separate the sine waves (see supplementary material for more details).

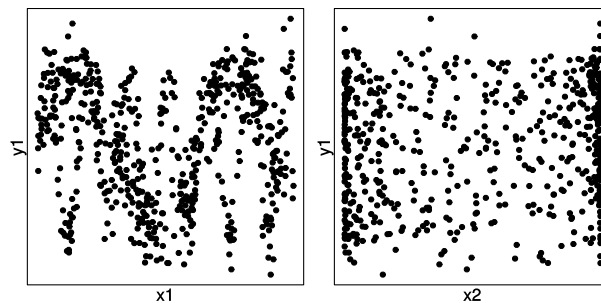


Figure 7: Marginal views of the superimposed sine setting. The X_1 - Y_1 margin (left) shows the superimposed sine waves.

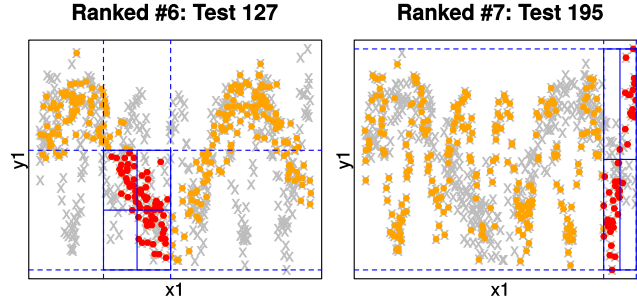


Figure 8: Tests for the superimposed sine setting with modified Holm’s adjusted p -values below 0.05. The testing was performed with Fisher’s exact test and the p -values presented here are modified Holm’s adjusted p -values. The tuning parameters were at their default. The first and third ranking tests identify the separate signals in the X_1 - Y plane, as determined by X_2 .

4 Application to a flow cytometry data set

Flow cytometry is the standard biological assay used to measure single cell features known as markers, and is commonly used to quantify the relative frequencies of cell subsets in blood or disaggregated tissue. These features may be general physical, chemical or biological properties of a cell.

For the evaluation, we used flow cytometry samples generated by an antibody panel designed to identify activated T cell subsets. We show the results of the dependency analysis on a single illustrative sample with 353,586 cells. For the analysis, we separated the markers into a vector of four ‘basic’ markers (dump, CD3, CD4, CD8) and a vector of four ‘functional’ markers (IFN, TNF, IL-2 and CD107). The basic markers are used in practice to first identify viable T cells by exclusion using the ‘dump’ and CD3 markers, and then to further partition T cells into CD4-positive (‘helper’) and CD8-positive (‘cytotoxic’) subsets. The functional markers are used to identify the activation status of these T cell subsets and their functional effector capabilities (IL-2 is a T cell growth factor, IFN and TNF are inflammatory cytokines, and CD107 is a component of the mechanism used by T cells to directly kill infected and cancer cells).

We applied the `MultiFIT` algorithm with Holm’s multiple testing adjustment. Our aim here is to demonstrate `MultiFIT`’s ability to handle such large data, and so we ran the

algorithm exhaustively up to the maximal resolution of 4 - testing 102,416 2×2 tables. The execution time of the algorithm in this setting is approximately 5 minutes on a laptop computer utilizing a single 3.00GHz Intel[®] Xeon(R) E3-1505M v6 CPU core. As the sample size is very large and the data clearly have strong marginal dependencies, **MultiFIT** identified hundreds of significant tests with p -values of machine zero. None of **HHG**, **DCov** and **dHSIC** was able to handle this amount of data and all ended in overflow errors. See also **Figure 3** for an illustration of the limits on the amount of data that each of the methods can handle in lower dimensions.

5 Conclusion

We have presented a scalable framework called **MultiFIT** for nonparametrically testing the independence of random vectors that achieves high computational scalability and statistical power. Very importantly, we provide a finite-sample theoretical guarantee for **MultiFIT** to control the FWER exactly without any resampling. This substantially broadens its applicability to large high-dimensional problems where resampling-based inference can be computationally prohibitive. **MultiFIT** excels in identifying non-linear and localized patterns of dependency, and provides insights as to the structure of detected dependencies. Our simulation studies have demonstrated that the estimated power of our algorithm compares favorably to that of the main competitors in many common scenarios, rendering our method a strong candidate for a wide variety of real life applications.

6 Acknowledgements

We thank Dr. Cliburn Chan for providing the flow cytometry data. The data is collected through an EQAPOL collaboration with federal funds from the National Institute of Allergy and Infectious Diseases, National Institutes of Health, Contract Number HHSN272201700061C.

7 Software

For the MultiFIT procedure we used our R package `MultiFit` on CRAN. For the Heller-Heller-Gorfine (HHG) test (Heller et al., 2013) we used the `HHG` package on CRAN. For Distance Covariance (`dCov`) (Székely and Rizzo, 2009) we used the `energy` package on CRAN. For `dHSIC` (Pfister et al., 2018) we used the `dHSIC` package on CRAN.

SUPPLEMENTARY MATERIAL

Proofs and additional simulation results: Proofs of all theorems and lemmas and additional simulation results that verify the FWER control (`supplement.pdf`)

R package: We have implemented an R package and made it freely available at <https://cran.r-project.org/web/packages/MultiFit/index.html>.

Source Code for Numerical Examples : Source code for the numerical examples from Section 3. (`numerical_examples.zip`)

Flow cytometry data set: Data set and code used in the illustration of MultiFIT in Section 4. (`flowcytometry.zip`)

References

- Agresti, A. and Gottard, A. (2007). Nonconservative exact small-sample inference for discrete data. *Computational Statistics & Data Analysis*, 51(12):6447 – 6458.
- Bakirov, N. K., Rizzo, M. L., and Székely, G. J. (2006). A multivariate nonparametric test of independence. *Journal of Multivariate Analysis*, 97:1742–1756.
- Fan, Y., de Micheaux, P. L., Penev, S., and Salopek, D. (2017). Multivariate nonparametric test of independence. *Journal of Multivariate Analysis*, 153:189–210.
- Gretton, A., Fukumizu, K., Teo, C. H., Song, L., Schölkopf, B., and Smola, A. J. (2008). A kernel statistical test of independence. In Platt, J. C., Koller, D., Singer, Y., and Roweis,

- S. T., editors, *Advances in Neural Information Processing Systems 20*, pages 585–592. Curran Associates, Inc.
- Heller, R., Heller, Y., and Gorfine, M. (2013). A consistent multivariate test of association based on ranks of distances. *Biometrika*, 100:503–510.
- Holm, S. (1979). A simple sequentially rejective multiple test procedure. *Scandinavian Journal of Statistics*, 6(2):65–70.
- Ma, L. and Mao, J. (2018). Fisher exact scanning for dependency. *Journal of the American Statistical Association*. Accepted.
- Meintanis, S. G. and Iliopoulos, G. (2008). Fourier methods for testing multivariate independence. *Computational Statistics & Data Analysis*, 52:1884–1895.
- Pfister, N., Bühlmann, P., Schölkopf, B., and Peters, J. (2018). Kernel-based tests for joint independence. *Journal of the Royal Statistical Society: Series B (Statistical Methodology)*, 80(1):5–31.
- Reshef, D. N., Reshef, Y. A., Finucane, H. K., Grossman, S. R., McVean, G., Turnbaugh, P. J., Lander, E. S., Mitzenmacher, M., and Sabeti, P. C. (2011). Detecting novel associations in large data sets. *Science*, 334(6062):1518–1524.
- Székely, G. J. and Rizzo, M. L. (2009). Brownian distance covariance. *The Annals of Applied Statistics*, 3(4):1236–1265.
- Székely, G. J. and Rizzo, M. L. (2013). The distance correlation t-test of independence in high dimension. *Journal of Multivariate Analysis*, 117:193 – 213.
- Wang, X., Jiang, B., and Liu, J. S. (2016). Generalized R-squared for detecting dependence. preprint.
- Weihs, L., Drton, M., and Meinshausen, N. (2018). Symmetric rank covariances: a generalized framework for nonparametric measures of dependence. *Biometrika*, 105(3):547–562.
- Zhang, K. (2017). BET on independence. preprint.

Zhu, Y. and Guo, W. (2017). Familywise error rate controlling procedures for discrete data.
preprint.

S1. Proofs

Proof of Theorem 2.1:

\Rightarrow : Immediate.

\Leftarrow :

Let $\mathcal{P}_x = \bigcup_{\mathbf{k}_{\{1, \dots, D_x\}} \in \mathbb{N}_0^{D_x}} \mathcal{P}^1 \times \dots \times \mathcal{P}^{D_x}$. Therefore $\sigma(\mathcal{P}_x) = \mathcal{B}([0, 1]^{D_x})$.

For $A_x \in \mathcal{B}([0, 1]^{D_x})$ let $[\mathbf{X} \in A_x] = \{\boldsymbol{\omega} : \mathbf{X}(\boldsymbol{\omega}) \in A_x\}$, then $\sigma(\mathbf{X}) = \{[\mathbf{X} \in A_x], A_x \in \mathcal{B}([0, 1]^{D_x})\}$.

Let $\mathcal{Q}_x = \bigcup_{\mathbf{k}_{\{1, \dots, D_x\}} \in \{-1, 0, 1, 2, \dots\}^{D_x}} \mathcal{Q}^{k_1} \times \dots \times \mathcal{Q}^{k_{D_x}}$ so that $\mathcal{Q}^{-1} := \emptyset$ and $\forall k \geq 0, \mathcal{Q}^k = \mathcal{P}^k$.

Let $\mathcal{C}_{\mathbf{X}} = \{[\mathbf{X} \in B_x], B_x \in \mathcal{Q}_x\}$.

Hence $\sigma(\mathcal{C}_{\mathbf{X}}) = \sigma(\mathbf{X}^{-1}(B_x), B_x \in \mathcal{Q}_x) = \sigma(\mathbf{X}^{-1}(\mathcal{Q}_x)) = \mathbf{X}^{-1}(\sigma(\mathcal{Q}_x)) = \mathbf{X}^{-1}(\sigma(\mathcal{P}_x)) = \sigma(\mathbf{X})$.

Note that $\mathcal{C}_{\mathbf{X}}$ is a π -system:

$E, E' \in \mathcal{C}_{\mathbf{X}} \Rightarrow E = \left[\mathbf{X} \in \left(\emptyset \text{ or } \left[\frac{l_1-1}{2^{k_1}}, \frac{l_1}{2^{k_1}} \right] \right) \times \dots \times \left(\emptyset \text{ or } \left[\frac{l_{D_x}-1}{2^{k_{D_x}}}, \frac{l_{D_x}}{2^{k_{D_x}}} \right] \right) \right]$ and
 $E' = \left[\mathbf{X} \in \left(\emptyset \text{ or } \left[\frac{l'_1-1}{2^{k'_1}}, \frac{l'_1}{2^{k'_1}} \right] \right) \times \dots \times \left(\emptyset \text{ or } \left[\frac{l'_{D_x}-1}{2^{k'_{D_x}}}, \frac{l'_{D_x}}{2^{k'_{D_x}}} \right] \right) \right]$ for some $\mathbf{l}, \mathbf{l}', \mathbf{k}, \mathbf{k}'$. Therefore:

$$\begin{aligned} E \cap E' &= \left[\mathbf{X} \in \left\{ \left(\emptyset \text{ or } \left[\frac{l_1-1}{2^{k_1}}, \frac{l_1}{2^{k_1}} \right] \right) \times \dots \times \left(\emptyset \text{ or } \left[\frac{l_{D_x}-1}{2^{k_{D_x}}}, \frac{l_{D_x}}{2^{k_{D_x}}} \right] \right) \right\} \cap \right. \\ &\quad \left. \left\{ \left(\emptyset \text{ or } \left[\frac{l'_1-1}{2^{k'_1}}, \frac{l'_1}{2^{k'_1}} \right] \right) \times \dots \times \left(\emptyset \text{ or } \left[\frac{l'_{D_x}-1}{2^{k'_{D_x}}}, \frac{l'_{D_x}}{2^{k'_{D_x}}} \right] \right) \right\} \right] \\ &= \left[\mathbf{X} \in \left(\emptyset \text{ or } \left[\frac{l_1-1}{2^{k_1}}, \frac{l_1}{2^{k_1}} \right] \cap \left[\frac{l'_1-1}{2^{k'_1}}, \frac{l'_1}{2^{k'_1}} \right] \right) \times \dots \right. \\ &\quad \left. \times \left(\left[\frac{l_{D_x}-1}{2^{k_{D_x}}}, \frac{l_{D_x}}{2^{k_{D_x}}} \right] \cap \left[\frac{l'_{D_x}-1}{2^{k'_{D_x}}}, \frac{l'_{D_x}}{2^{k'_{D_x}}} \right] \right) \right] \in \mathcal{C}_{\mathbf{X}} \end{aligned}$$

Similarly, define $\sigma(\mathbf{Y})$ and $\mathcal{C}_{\mathbf{Y}}$, another π -system, independent of $\mathcal{C}_{\mathbf{X}}$ and $\sigma(\mathbf{Y}) = \sigma(\mathcal{C}_{\mathbf{Y}})$.

By the basic criterion, then, $\sigma(\mathbf{X}) \perp \sigma(\mathbf{Y})$.

For the rest of this section we adopt the following notations:

Denote $X_1 = Z_1, \dots, X_{D_x} = Z_{D_x}$ and $Y_1 = Z_{D_x+1}, \dots, Y_{D_y} = Z_D$.

$\mathbf{d} \subset \{1, \dots, D\}$, $\mathbf{i} = \mathbf{d} \cap \{1, \dots, D_x\}$ and $\mathbf{j} = \{j : j + D_x \in \mathbf{d} \cap \{D_x + 1, \dots, D\}\}$

Denote

$$\begin{aligned} \mathbf{X}_{\mathbf{i}} &= \{X_i : i \in \mathbf{i}\}, & \mathbf{X}_{(\mathbf{i})} &= \{X_{i'} : i' \in \{1, \dots, D_x\} \setminus \mathbf{i}\} \\ \mathbf{Y}_{\mathbf{j}} &= \{Y_j : j \in \mathbf{j}\}, & \mathbf{Y}_{(\mathbf{j})} &= \{Y_{j'} : j' \in \{1, \dots, D_y\} \setminus \mathbf{j}\} \\ \mathbf{Z}_{\mathbf{d}} &= \mathbf{X}_{\mathbf{i}} \times \mathbf{Y}_{\mathbf{j}} = \{Z_d : d \in \mathbf{d}\}, & \mathbf{Z}_{(\mathbf{d})} &= \mathbf{X}_{(\mathbf{i})} \times \mathbf{Y}_{(\mathbf{j})} = \{Z_{d'} : d' \in \{1, \dots, D\} \setminus \mathbf{d}\} \end{aligned}$$

$$\begin{aligned} A_{x, \mathbf{d}} &= \bigtimes_{d \in \mathbf{d} \cap \{1, \dots, D_x\}} A_d, & A_{x, (\mathbf{d})} &= \bigtimes_{d' \in \{1, \dots, D_x\} \setminus \mathbf{d}} A_{d'} \\ A_{y, \mathbf{d}} &= \bigtimes_{d \in \mathbf{d} \cap \{D_x + 1, \dots, D\}} A_d, & A_{y, (\mathbf{d})} &= \bigtimes_{d' \in \{D_x + 1, \dots, D\} \setminus \mathbf{d}} A_{d'} \\ A_{\mathbf{d}} &= A_{x, \mathbf{d}} \times A_{y, \mathbf{d}} = \bigtimes_{d \in \mathbf{d}} A_d, & A_{(\mathbf{d})} &= A_{x, (\mathbf{d})} \times A_{y, (\mathbf{d})} = \bigtimes_{d' \in \{1, \dots, D\} \setminus \mathbf{d}} A_{d'} \end{aligned}$$

$$\mathbf{k}_{\mathbf{d}} = \{k_d : d \in \mathbf{d}\}, \quad \mathbf{k}_{(\mathbf{d})} = \{k_{d'} : d' \in \{1, \dots, D\} \setminus \mathbf{d}\}$$

Definition 7.1. *Conditional \mathbf{k} -independence:*

We say that $\mathbf{X}_{\mathbf{i}}$ and $\mathbf{Y}_{\mathbf{j}}$ are \mathbf{k} -independent conditional on $\mathbf{Z}_{(\mathbf{d})}$ and write it as $\mathbf{X}_{\mathbf{i}} \perp_{\mathbf{k}} \mathbf{Y}_{\mathbf{j}} \mid \mathbf{Z}_{(\mathbf{d})}$ if for any $A \in \mathcal{A}^{\mathbf{k}}$:

$$\mathbb{P}(\mathbf{X}_{\mathbf{i}} \in A_{x, \mathbf{d}}, \mathbf{Y}_{\mathbf{j}} \in A_{y, \mathbf{d}} \mid \mathbf{Z}_{(\mathbf{d})} \in A_{(\mathbf{d})}) = \mathbb{P}(\mathbf{X}_{\mathbf{i}} \in A_{x, \mathbf{d}} \mid \mathbf{Z}_{(\mathbf{d})} \in A_{(\mathbf{d})}) \cdot \mathbb{P}(\mathbf{Y}_{\mathbf{j}} \in A_{y, \mathbf{d}} \mid \mathbf{Z}_{(\mathbf{d})} \in A_{(\mathbf{d})})$$

Or equivalently:

$$\mathbb{P}(\mathbf{X}_{\mathbf{i}} \in A_{x, \mathbf{d}} \mid \mathbf{Y}_{\mathbf{j}} \in A_{y, \mathbf{d}}, \mathbf{Z}_{(\mathbf{d})} \in A_{(\mathbf{d})}) = \mathbb{P}(\mathbf{X}_{\mathbf{i}} \in A_{x, \mathbf{d}} \mid \mathbf{Z}_{(\mathbf{d})} \in A_{(\mathbf{d})})$$

When $k_{d'} = 0$ for some $d' \in \{1, \dots, D\} \setminus \mathbf{d}$, $\Omega_{Z_{d'}} = [0, 1]$ for those indices and hence our notation may be compacted. For example, if $k_{d'} = 0$ for all $d' \in \{1, \dots, D\} \setminus \mathbf{d}$:

$$\mathbf{X}_{\mathbf{i}} \perp_{\mathbf{k}} \mathbf{Y}_{\mathbf{j}} \mid \mathbf{Z}_{(\mathbf{d})} \Leftrightarrow \mathbf{X}_{\mathbf{i}} \perp_{\mathbf{k}_{\mathbf{d}}} \mathbf{Y}_{\mathbf{j}}$$

Definition 7.2. For $A_d \in \mathcal{P}^{k_d - 1}$ such that $A_d = \left[\frac{l_d - 1}{2^{k_d - 1}}, \frac{l_d}{2^{k_d - 1}} \right)$, define $A_d^0 = \left[\frac{2l_d - 2}{2^{k_d}}, \frac{2l_d - 1}{2^{k_d + 1}} \right) \in \mathcal{P}^{k_d}$ and

$$A_d^1 = \left[\frac{2l_d - 1}{2^{k_d + 1}}, \frac{2l_d}{2^{k_d + 1}} \right) \in \mathcal{P}^{k_d}. \text{ Note that } A_d = A_d^0 \sqcup A_d^1.$$

Proof of Lemma 2.1:

Let $F_{\mathbf{X}}$ be the probability distribution of \mathbf{X} and $F_{\mathbf{Y}}$ be the probability distribution of \mathbf{Y} .

Then $\mathbf{X} \perp_{\mathbf{k}} \mathbf{Y} \Leftrightarrow F(A) = F_{\mathbf{X}}(A_x)F_{\mathbf{Y}}(A_y)$ for all $A \in \mathcal{A}^{\mathbf{k}}$.

It is enough to show that $\mathbf{X} \perp_{\mathbf{k}} \mathbf{Y} \Rightarrow \mathbf{X} \perp_{\mathbf{k}'} \mathbf{Y}$ for any \mathbf{k}' such that (i) $k'_i = k_i - 1$ for some $i \in \{1, \dots, D_x\}$ and (ii) $k'_d = k_d$ for all $d \in \{1, \dots, D\} \setminus \{i\}$.

Hence, assuming $\mathbf{X} \perp_{\mathbf{k}} \mathbf{Y}$ we get for $A \in \mathcal{A}^{\mathbf{k}'}$ that:

$$\begin{aligned} F(A) &= F(A_1 \times \dots \times A_{i-1} \times A_i^0 \times A_{i+1} \times \dots \times A_{D_x} \times A_y) \\ &\quad + F(A_1 \times \dots \times A_{i-1} \times A_i^1 \times A_{i+1} \times \dots \times A_{D_x} \times A_y) \\ &= F_{\mathbf{X}}(A_1 \times \dots \times A_{i-1} \times A_i^0 \times A_{i+1} \times \dots \times A_{D_x}) F_{\mathbf{Y}}(A_y) \\ &\quad + F_{\mathbf{X}}(A_1 \times \dots \times A_{i-1} \times A_i^1 \times A_{i+1} \times \dots \times A_{D_x}) F_{\mathbf{Y}}(A_y) \\ &= F_{\mathbf{X}}(A_x) F_{\mathbf{Y}}(A_y) \end{aligned}$$

As required.

We next provide a discretized version of some basic results in probability:

Lemma 7.1. Contraction:

For $\mathbf{d} \subset \{1, \dots, D\}$ such that $\{1, \dots, D_x\} \subset \mathbf{d}$ (i.e. $\mathbf{i} = \{1, \dots, D_x\}$, $\mathbf{X}_{\mathbf{i}} = \mathbf{X}$ and $\mathbf{Y}_{(\mathbf{j})} = \mathbf{Z}_{(\mathbf{d})}$):

$$\begin{cases} \mathbf{X} \perp_{\mathbf{k}} \mathbf{Y}_{\mathbf{j}} \mid \mathbf{Z}_{(\mathbf{d})} \\ \mathbf{X} \perp_{\mathbf{k}_{(\mathbf{d})}} \mathbf{Y}_{(\mathbf{j})} \end{cases} \Rightarrow \mathbf{X} \perp_{\mathbf{k}} \mathbf{Y}$$

Proof: Immediate from definition.

Lemma 7.2. Decomposition:

For $\mathbf{d} \subset \{1, \dots, D\}$ such that $\{1, \dots, D_x\} \subset \mathbf{d}$ (i.e. $\mathbf{i} = \{1, \dots, D_x\}$ and $\mathbf{X}_{\mathbf{i}} = \mathbf{X}$):

$$\mathbf{X} \perp_{\mathbf{k}} \mathbf{Y} \Rightarrow \begin{cases} \mathbf{X} \perp_{\mathbf{k}_{\mathbf{d}}} \mathbf{Y}_{\mathbf{j}} \\ \mathbf{X} \perp_{\mathbf{k}_{(\mathbf{d})}} \mathbf{Y}_{(\mathbf{j})} \end{cases}$$

Proof: Immediate from definition.

Lemma 7.3. Weak Union:

For $\mathbf{d} \subset \{1, \dots, D\}$ such that $\{1, \dots, D_x\} \subset \mathbf{d}$ (i.e. $\mathbf{i} = \{1, \dots, D_x\}$, $\mathbf{X}_{\mathbf{i}} = \mathbf{X}$, $\mathbf{Y}_{\mathbf{j}} = \mathbf{Z}_{\mathbf{d}}$ and

$\mathbf{Y}_{(j)} = \mathbf{Z}_{(d)}$:

$$\mathbf{X} \perp_{\mathbf{k}} \mathbf{Y} \Rightarrow \begin{cases} \mathbf{X} \perp_{\mathbf{k}} \mathbf{Y}_j \mid \mathbf{Z}_{(d)} \\ \mathbf{X} \perp_{\mathbf{k}} \mathbf{Y}_{(j)} \mid \mathbf{Z}_d \end{cases}$$

Proof: Immediate from definition.

Definition 7.3. Given $\mathbf{k} \in \mathbb{N}_0^D$ and $i \in \{1, \dots, D_x\}$, $j \in \{1, \dots, D_y\}$ let

$$\begin{aligned} [k_i, k_j](\mathbf{k}_{<i, <j}) &= \{\mathbf{k}' \in \mathbb{N}_0^D : && k'_i < k_i, k'_j < k_j \text{ and} \\ &&& k'_d = k_d \text{ for all } d \in \{1, \dots, i-1\} \cup \{D_x+1, \dots, D_x+j-1\} \\ &&& \text{and} \\ &&& k'_d = 0 \text{ for all } d \in \{i+1, \dots, D_x\} \cup \{D_x+j+1, \dots, D\}\} \end{aligned}$$

Accordingly,

$$\mathcal{A}^{[k_i, k_j](\mathbf{k}_{<i, <j})} = \bigcup_{\mathbf{k}' \in [k_i, k_j](\mathbf{k}_{<i, <j})} \mathcal{A}^{\mathbf{k}'}$$

denote the totality of all cuboids in strata that are coarser than the stratum $\mathcal{A}^{\mathbf{k}}$ along the margins i and j such that margins $\{i+1, \dots, D_x\}$ and $\{D_x+j+1, \dots, D\}$ are allowed any value in $[0, 1]$.

Proof of Theorem 2.2:

\Rightarrow :

Assume $\mathbf{X} \perp_{\mathbf{k}} \mathbf{Y}$ for some $\mathbf{k} \in \mathbb{N}_0^D$.

Let $i \in \{1, \dots, D_x\}$ and $j \in \{1, \dots, D_y\}$.

By applying the weak union lemma twice we get that $X_i \perp_{(k_i, k_{D_x+j})} Y_j \mid \mathbf{Z}_{(\{i, D_x+j\})}$.

Notice that for \mathbf{k}' such that $k'_i = k_i - 1$, $k'_{D_x+j} = k_{D_x+j} - 1$, $k'_d = k_d$ for all $d \in \{1, \dots, D\} \setminus \{i, D_x+j\}$ and $A \in \mathcal{A}^{\mathbf{k}'}$ we get that $A_{ij}^{00}, A_{ij}^{11}, A_{ij}^{01}, A_{ij}^{10} \in \mathcal{A}^{\mathbf{k}}$. So $\theta_{ij}(A) = 0$ by the definition of conditional independence and the LOR.

By Lemma 2.1 we get that indeed $\theta_{ij}(A) = 0$ for $A \in \mathcal{A}^{[k_i, k_j]}$.

\Leftarrow :

First, notice that it suffices to show that:

$$\begin{aligned} \mathbf{X} \perp_{\mathbf{k}} \mathbf{Y} &\Leftarrow \theta_{ij}(A) = 0 \\ &\forall i \in \{1, 2, \dots, D_x\}, \quad j \in \{D_x+1, \dots, D\}, \quad A \in \mathcal{A}^{[k_i, k_j](\mathbf{k}_{<i, <j})} \end{aligned}$$

Since then we may rely on the opposite direction to get that $\theta_{ij}(A) = 0$ for all $A \in \mathcal{A}^{[k_i, k_j]}$.

Examine

$$X_i \perp\!\!\!\perp_{\mathbf{k}_{\{1, \dots, i, D_x+1, \dots, D_x+j\}}} Y_j \mid \mathbf{X}_{\{1, \dots, i-1\}}, \mathbf{Y}_{\{1, \dots, j-1\}}$$

To see that the above is true, let $\mathbf{k}' \in \mathbb{N}_0^D$ such that $k'_d = k_d$ for all $d \in \{1, \dots, i\} \cup \{D_x + 1, \dots, D_x + j\}$ and

$k'_d = 0$ for all $d \in \{i + 1, \dots, D_x\} \cup \{D_x + j + 1, \dots, D\}$.

For a given $A \in \mathcal{A}^{\mathbf{k}'}$ let x, y be a pair of univariate random variables whose joint distribution is given by $G := F_{X_i, Y_j \mid \mathbf{X}_{\{1, \dots, i-1\}} \in A_x, \{1, \dots, i-1\}, \mathbf{Y}_{\{1, \dots, j-1\}} \in A_y, \{D_x+1, \dots, D_x+j-1\}}$. By assumption:

$$\begin{aligned} 0 = \theta_{ij}(A) &= \log \frac{F(A_{ij}^{00}) \cdot F(A_{ij}^{11})}{F(A_{ij}^{01}) \cdot F(A_{ij}^{10})} \\ &= \log \frac{G(A_i^0 \times A_{D_x+j}^0) \cdot G(A_i^1 \times A_{D_x+j}^1)}{G(A_i^0 \times A_{D_x+j}^1) \cdot G(A_i^1 \times A_{D_x+j}^0)} \end{aligned}$$

Since the above holds for every $A \in \mathcal{A}^{[k_i, k_j](\mathbf{k}_{<i, <j})}$ we may apply Theorem 2 from Ma and Mao (2018) and conclude that $x \perp\!\!\!\perp_{(k_i, k_{D_x+j})} y$ which is equivalent to $X_i \perp\!\!\!\perp_{\mathbf{k}_{\{1, \dots, i, D_x+1, \dots, D_x+j\}}} Y_j \mid \mathbf{X}_{\{1, \dots, i-1\}}, \mathbf{Y}_{\{1, \dots, j-1\}}$.

Next, examine:

$$\begin{aligned}
(\star) & \left\{ \begin{array}{l} X_1 \perp\!\!\!\perp_{\mathbf{k}_{\{1, D_x+1\}}} Y_1 \\ X_1 \perp\!\!\!\perp_{\mathbf{k}_{\{1, D_x+1, D_x+2\}}} Y_2 \mid Y_1 \\ X_1 \perp\!\!\!\perp_{\mathbf{k}_{\{1, D_x+1, D_x+2, D_x+3\}}} Y_3 \mid \mathbf{Y}_{\{1,2\}} \\ \vdots \\ X_1 \perp\!\!\!\perp_{\mathbf{k}_{\{1, D_x+1, \dots, D-1\}}} Y_{D_y-1} \mid \mathbf{Y}_{\{1, \dots, D_y-2\}} \\ X_1 \perp\!\!\!\perp_{\mathbf{k}_{\{1, D_x+1, \dots, D\}}} Y_{D_y} \mid \mathbf{Y}_{\{1, \dots, D_y-1\}} \end{array} \right. \\
(\star\star) & \left\{ \begin{array}{l} X_2 \perp\!\!\!\perp_{\mathbf{k}_{\{1,2, D_x+1\}}} Y_1 \mid X_1 \\ X_2 \perp\!\!\!\perp_{\mathbf{k}_{\{1,2, D_x+1, D_x+2\}}} Y_2 \mid X_1, Y_1 \\ \vdots \\ X_2 \perp\!\!\!\perp_{\mathbf{k}_{\{1,2, D_x+1, \dots, D\}}} Y_{d_y} \mid X_1, \mathbf{Y}_{\{1, \dots, D_y-1\}} \\ \vdots \end{array} \right. \\
(\star\star\star) & \left\{ \begin{array}{l} X_{D_x} \perp\!\!\!\perp_{\mathbf{k}_{\{1, \dots, D_x, D_x+1\}}} Y_1 \mid \mathbf{X}_{\{1, \dots, D_x-1\}} \\ X_{D_x} \perp\!\!\!\perp_{\mathbf{k}_{\{1, \dots, D_x, D_x+1, D_x+2\}}} Y_2 \mid \mathbf{X}_{\{1, \dots, D_x-1\}}, Y_1 \\ \vdots \\ X_{D_x} \perp\!\!\!\perp_{\mathbf{k}} Y_{D_y} \mid \mathbf{X}_{\{1, \dots, D_x-1\}}, \mathbf{Y}_{\{1, \dots, D_y-1\}} \end{array} \right.
\end{aligned}$$

Each of the above rows is obtained by the previous argument. Applying the contraction lemma recursively from top to bottom to each of the rows in (\star) shows that $X_1 \perp\!\!\!\perp_{\{1, D_x, \dots, D\}} \mathbf{Y}$. Further applying the contraction lemma to the latter result and the rows of $(\star\star)$ shows that $\mathbf{X}_{\{1,2\}} \perp\!\!\!\perp_{\{1,2, D_x, \dots, D\}} \mathbf{Y}$. And a similar application of the contraction lemma to the previous results and all the rows up to $(\star\star\star)$ shows that $\mathbf{X} \perp\!\!\!\perp_{\mathbf{k}} \mathbf{Y}$. \square

Note, for every $i \in \{1, \dots, D_x\}$ and $j \in \{1, \dots, D_y\}$, and for each of the above conditions $X_i \perp\!\!\!\perp_{\mathbf{k}_{\{1, \dots, i-1, D_x+1, \dots, D_x+j\}}} Y_j \mid \mathbf{X}_{\{1, \dots, i-1\}}, \mathbf{Y}_{\{1, \dots, j-1\}}$ there are $(2^{k_i} - 1)(2^{k_j} - 1)$ one degrees of freedom tests required, each repeated due to the conditioning $\prod_{s=1}^{i-1} 2^{k_s} \cdot \prod_{t=D_x+1}^{D-1} 2^{k_t}$ times. Summing over j , we get that for each i , there are $(2^{k_i} - 1) \cdot \prod_{s=1}^{i-1} 2^{k_s} \cdot (2^{\sum_{t=D_x+1}^D k_t} - 1)$ one degrees of freedom tests. Summing those over i we get that overall we need to perform $(2^{\sum_{s=1}^{D_x} k_s} - 1)(2^{\sum_{t=D_x+1}^D k_t} - 1)$ one degrees of freedom tests.

Under H_1 there are $2^{\sum_{s=1}^{D_x} k_s} \cdot 2^{\sum_{t=D_x+1}^D k_t} - 1$ degrees of freedom, under H_0 there are $(2^{\sum_{s=1}^{D_x} k_s} - 1) + (2^{\sum_{t=D_x+1}^D k_t} - 1)$ degrees of freedom, and thus we need $(2^{\sum_{s=1}^{D_x} k_s} - 1)(2^{\sum_{t=D_x+1}^D k_t} - 1)$ degrees of freedom to identify a difference between the null and the alternative. It follows from the proof that we may indeed use $(2^{\sum_{s=1}^{D_x} k_s} - 1)(2^{\sum_{t=D_x+1}^D k_t} - 1)$ 1-degree of freedom independence tests to do so.

Proof of Theorem 2.3:

Let A be a cuboid in resolution r . For any $r > R^*$, whether for not A is selected in the `MultiFIT` procedure for testing is determined by the p -values observed on the collection of all potential ancestral cuboids of A . Without loss of generality we let $R^* = 0$ to simplify notation. The general case requires trivial changes to the proof. A cuboid A will be selected in `MultiFIT` if there exists a sequence of nested cuboids, or a lineage, $A_0 \subset A_1 \subset \dots \subset A_r$ of resolution $0, 1, \dots, r$ respectively such that each A_{k+1} is a child cuboid of A_k in the (i_k, j_k) -face, and moreover, the p -value of the (i_k, j_k) -table of A_k is less than the threshold p^* . As such, the event that a cuboid A is in $\mathcal{C}^{(r)}$ is in the σ -algebra generated by the 2×2 -table counts $\mathbf{n}(\bar{A}_{ij})$ for all (i, j) pairs and all sets \bar{A} that can be an ancestor cuboid of A along some lineage.

Suppose the resolution- r cuboid A is in the $\mathcal{A}^{\mathbf{k}}$ stratum with $|\mathbf{k}| = \sum_{d=1}^D k_d = r$. Also, let $r_x = \sum_{d=1}^{D_x} k_d$ and $r_y = \sum_{d=D_x+1}^D k_d$. Any potential ancestor cuboid of A , denoted by \bar{A} , is the union of several sets in $\mathcal{A}^{\mathbf{k}}$, and thus the (i, j) -table of \bar{A} , $\mathbf{n}(\bar{A}_{ij})$, for every (i, j) pair, is determined exactly if we know the counts in all sets in $\mathcal{A}^{\mathbf{k}}$.

For any positive integer ρ , we denote the collection of all level- ρ marginal partition of $\Omega_{\mathbf{X}}$ as

$$\tilde{\mathcal{P}}_x^\rho = \left\{ \mathcal{P}^{k_1} \times \dots \times \mathcal{P}^{k_{D_x}} : \sum_{d=1}^{D_x} k_d = \rho \right\}$$

and the collection of all level- ρ marginal partition of $\Omega_{\mathbf{Y}}$ as

$$\tilde{\mathcal{P}}_y^\rho = \left\{ \mathcal{P}^{k_{D_x+1}} \times \dots \times \mathcal{P}^{k_D} : \sum_{d=D_x+1}^D k_d = \rho \right\}$$

Consider the following sequence of nested marginal partitions on $\Omega_{\mathbf{X}}$, $\tilde{\mathcal{P}}_x^1 \subset \tilde{\mathcal{P}}_x^2 \subset \dots \subset \tilde{\mathcal{P}}_x^{r_x} \subset \tilde{\mathcal{P}}_x^{r_x+1} \subset \tilde{\mathcal{P}}_x^{r_x+2} \subset \dots \subset \tilde{\mathcal{P}}_x^{r_x+D_x}$ (where $\tilde{\mathcal{P}}_x^1 \in \tilde{\mathcal{P}}_x^1, \dots, \tilde{\mathcal{P}}_x^{r_x+D_x} \in \tilde{\mathcal{P}}_x^{r_x+D_x}$), such that we first divide X_1 k_1 times to get $\tilde{\mathcal{P}}_x^1, \dots, \tilde{\mathcal{P}}_x^{k_1}$, followed by dividing X_2 k_2 times to get $\tilde{\mathcal{P}}_x^{k_1+1}, \dots, \tilde{\mathcal{P}}_x^{k_1+k_2}$, and so on an so forth until dividing X_{D_x} k_{D_x} times to get

$\tilde{\mathcal{P}}_x^{r_x - k_{D_x} + 1}, \dots, \tilde{\mathcal{P}}_x^{r_x}$. Then one divides X_i once to get $\tilde{\mathcal{P}}_x^{r_x + 1}$, finally divide each of the other $D_x - 1$ dimensions once in any order to get $\tilde{\mathcal{P}}_x^{r_x + 2}, \dots, \tilde{\mathcal{P}}_x^{r_x + D_x}$.

In exactly the same manner, we can construct a sequence of nested marginal partitions of $\Omega_{\mathbf{Y}}$, $\tilde{\mathcal{P}}_y^1 \subset \tilde{\mathcal{P}}_y^2 \subset \dots \subset \tilde{\mathcal{P}}_y^{r_y} \subset \tilde{\mathcal{P}}_y^{r_y + 1} \subset \tilde{\mathcal{P}}_y^{r_y + 2} \subset \dots \subset \tilde{\mathcal{P}}_y^{r_y + D_y}$ (where $\tilde{\mathcal{P}}_y^1 \in \tilde{\mathcal{P}}_y^1, \dots, \tilde{\mathcal{P}}_y^{r_y + D_y} \in \tilde{\mathcal{P}}_y^{r_y + D_y}$) such that we first divide Y_1 $k_{D_x + 1}$ times to get $\tilde{\mathcal{P}}_y^1, \dots, \tilde{\mathcal{P}}_y^{k_{D_x + 1}}$, followed by dividing Y_2 $k_{D_x + 2}$ times to get $\tilde{\mathcal{P}}_y^{k_{D_x + 1} + 1}, \dots, \tilde{\mathcal{P}}_y^{k_{D_x + 1} + k_{D_x + 2}}$, and so on an so forth until dividing Y_{D_y} k_D times to get $\tilde{\mathcal{P}}_y^{r_y - k_D + 1}, \dots, \tilde{\mathcal{P}}_y^{r_y}$. Then one divides Y_j once to get $\tilde{\mathcal{P}}_y^{r_y + 1}$, finally divide each of the other $D_y - 1$ dimensions once in any order to get $\tilde{\mathcal{P}}_x^{r_x + 1}, \dots, \tilde{\mathcal{P}}_x^{r_x + D_y}$.

Under these two marginal partition sequences, we have $A \in \tilde{\mathcal{P}}_x^{r_x} \times \tilde{\mathcal{P}}_y^{r_y} = \mathcal{A}^{\mathbf{k}}$, whereas the four child cuboids of A with respect to the (i, j) -face are in the two strata $\tilde{\mathcal{P}}_x^{r_x + 1} \times \tilde{\mathcal{P}}_y^{r_y}$ and $\tilde{\mathcal{P}}_x^{r_x} \times \tilde{\mathcal{P}}_y^{r_y + 1}$. Moreover, any (i, j) -face of any ancestral cuboid of A are formed by unions of sets that are not in the strata $\tilde{\mathcal{P}}_x^{r_x + i'} \times \tilde{\mathcal{P}}_y^{r_y + j'}$ for $i' = 1, 2, \dots, D_x$ and $j' = 1, 2, \dots, D_y$.

Now by Theorem 3 in Ma and Mao (2018), conditional on the \mathbf{X} and \mathbf{Y} marginal values of the observations, the counts in any (i, j) -table of A given the corresponding row and column totals are independent of the σ -algebra generated by all counts in the sets that are not of the form $\tilde{\mathcal{P}}_x^{r_x + i'} \times \tilde{\mathcal{P}}_y^{r_y + j'}$ for $i' = 1, 2, \dots, D_x$ and $j' = 1, 2, \dots, D_y$. Therefore, the counts in any (i, j) -table of A are also independent of the σ -algebra generated by the 2×2 -table counts $\mathbf{n}(\bar{A}_{ij})$ for all sets \bar{A} that can be ancestor cuboids of A along some lineage and all (i, j) pairs, and hence also independent of the selection under the **MultiFIT** procedure. The ideas of the proof are illustrated in Figure S1. \square

Proof of Corollary 2.1:

This corollary follows immediately since the p -value on the (i, j) -table of a cuboid A is determined from the (central) hypergeometric distribution given the row and column totals of that table, which due to Theorem 2.3, is the actual sampling distribution of the table given the row and column totals under the null hypothesis of independence whether or not one conditions on the event that A is selected for testing in the **MultiFIT** procedure.

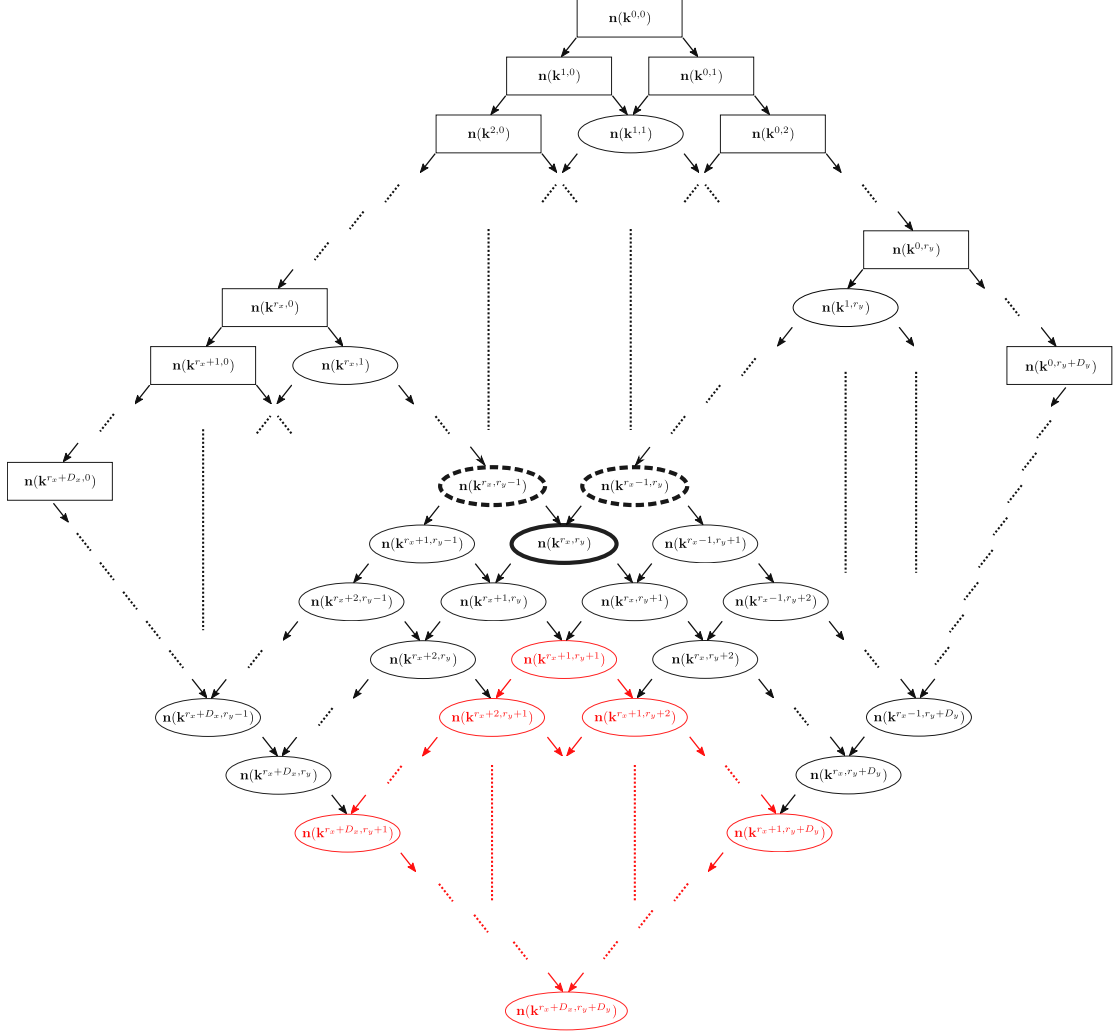


Figure S1: For any $\mathbf{k} = (k_1, \dots, k_D)$, $\mathbf{n}(\mathbf{k}) = \{n(A) : A \in \mathcal{A}^{\mathbf{k}}\}$ represents the $2^{\sum_{d=1}^{D_x} k_d} \times 2^{\sum_{d=D_x+1}^D k_d}$ contingency table corresponding to the \mathbf{k} -stratum. Also, for $\rho_x = 0, 1, \dots, r_x + D_x$ and $\rho_y = 0, 1, \dots, r_y + D_x$, we let $\mathbf{k}^{\rho_x, \rho_y}$ be the vector that corresponds to the stratum formed by the two marginal partitions $\tilde{\mathcal{P}}_x^{\rho_x}$ and $\tilde{\mathcal{P}}_y^{\rho_y}$. That is, $\mathcal{A}^{\mathbf{k}^{\rho_x, \rho_y}} = \tilde{\mathcal{P}}_x^{\rho_x} \times \tilde{\mathcal{P}}_y^{\rho_y}$. Theorem 3 in Ma and Mao (2018) shows that the generative model for the contingency table $\mathbf{n}(\mathbf{k}^{r_x+D_x, r_y+D_y})$ given the marginal values can be represented by the above Bayesian network. (The rectangular nodes are non-random given the marginal values of the observations while the elliptical nodes are random variables.) Therefore, any (i, j) -face of any ancestral cuboid of $A \in \mathcal{A}^{\mathbf{k}^{r_x, r_y}}$ are formed by unions of sets that are not in the strata marked in red. Conditional on the \mathbf{X} and \mathbf{Y} marginal values of the observations, the counts in any (i, j) -table of A given the corresponding row and column totals are independent of the σ -algebra generated by all counts in the sets that are not marked in red, under which the event that the set A is selected in **MultiFIT** is measurable.

S2. Estimating FWER through simulations

To demonstrate that MultiFIT properly controls the FWER we executed 2,000 simulations with the default tuning parameters for various sample sizes. The underlying data $\{X_{1i}\}$, $\{X_{2i}\}$, $\{Y_{1i}\}$ and $\{Y_{2i}\}$ are drawn independently from a standard normal distribution for $i \in \{1, \dots, n\}$ with $n \in \{100, 200, \dots, 2000\}$. **Figure S2** shows the estimated FWER for MultiFIT with different variations for the independence tests on each table and multiple testing adjustment options: Fisher’s exact test, Fisher’s exact test with mid- p corrected p -values (see Agresti and Gottard (2007) for a discussion on the mid- p correction), Fisher’s exact test with a modified Holm correction of Zhu and Guo (2017) and an approximation for Fisher’s exact test based on the normal approximation of the central hypergeometric distribution with Holm’s multiple testing adjustment.

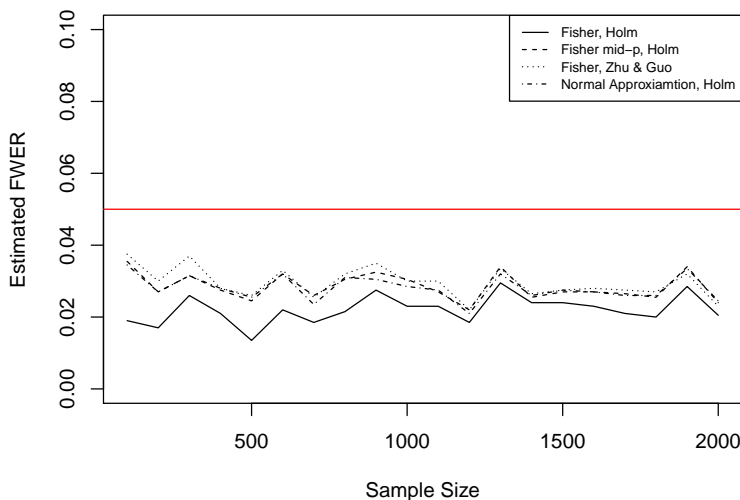


Figure S2: Estimated FWER

The results confirm the theoretical guarantees that the FWER can be controlled at any given level α . In fact the procedure appears to be a bit conservative in controlling the FWER. Note, although \mathbf{X} and \mathbf{Y} are independent under the null hypothesis, the dependency structure between the different margins of \mathbf{X} is arbitrary, as well as the dependency structure between the different margins of \mathbf{Y} . Therefore, this simulation is not exhaustive. However, we repeated the estimation of the FWER under various dependency structures for the margins, and the results are consistent with these that are shown here.